Chemical Science

ROYAL SOCIETY OF CHEMISTRY

EDGE ARTICLE

View Article Online
View Journal | View Issue

Cite this: *Chem. Sci.*, 2025, **16**, 6930

All publication charges for this article have been paid for by the Royal Society of Chemistry

Leveraging heterocycle-fused 1,4-benzoquinone to design chemical modulators for both metal-free and metal-bound amyloid-β†

Yelim Yi, [a] Kyungmin Kim, [b] Hakwon Kim *[b] and Mi Hee Lim *[a]

The complex pathology of Alzheimer's disease includes various pathogenic components, such as metal-free amyloid-β (Aβ) and metal-bound Aβ (metal–Aβ). Here we report an effective strategy for developing novel heterocycle-fused 1,4-benzoquinone (**BQ**) compounds to control the aggregation and toxicity of both metal-free Aβ and metal–Aβ. We designed and synthesized these compounds by fusing **BQ** with 3-pyrazolone responsible for metal chelation. The compounds' ability to form covalent bonds with Aβ is tuned by the annulation of the **BQ** moiety and the type, position, and number of substituents on the 3-pyrazolone group. Furthermore, the **BQ** functionality on the 3-pyrazolone framework can undergo *o*-hydroxylation, enhancing its metal chelation in a bidentate manner. Our results demonstrate that these heterocycle-fused **BQ** compounds can redirect the assembly of Aβ into less toxic aggregates by binding to metal ions, modifying Aβ structures in both the absence and presence of metal ions, and promoting oxidative changes to Aβ. This study highlights the importance of structural modifications and optimizations of **BQ** to leverage its strength of covalently cross-linking to Aβ and overcome its limitations in metal chelation and cytotoxicity, which are critical for designing chemical modulators for metal-free Aβ and metal–Aβ. Our approach offers a novel strategy for developing chemical modulators towards metal-related peptides and proteins as well as therapeutic agents for metal-associated amyloid disorders.

Received 8th September 2024
Accepted 11th March 2025

DOI: 10.1039/d4sc06070a

rsc.li/chemical-science

Introduction

Aberrant aggregation of peptides and proteins is linked to numerous pathological conditions.[1] The amyloid cascade hypothesis, which suggests that the accumulation of amyloid-β (Aβ) aggregates is a primary cause of Alzheimer's disease (AD), has been extensively studied. This has led to the development of various chemical tools and therapeutic agents aimed at targeting and modulating Aβ aggregation.[2,3] Notably, Aβ-directed monoclonal antibodies have been approved by the United States Food and Drug Administration as AD treatment, although concerns about their efficacy and safety persist.[4,5] This underscores the importance of the amyloid paradigm in understanding the pathology of AD while highlighting the need for further investigation into other biological factors influencing Aβ aggregation profiles.[6,7] High concentrations of metal ions, such as Cu(I/II) and Zn(II), are found in Aβ aggregates in the brains of AD patients.[8–16] Metal coordination to Aβ peptides affects their conformation and aggregation pathways, indicating metal-bound Aβ (metal–Aβ) as an additional pathological component of AD.[9–21] Therefore, developing chemical reagents that can modulate both metal-free Aβ and metal–Aβ is crucial for addressing the complex pathology of AD.

As a means of modifying the aggregation profiles of Aβ, the manipulation of amino acid residues in the peptides has been reported.[22–25] As shown in Fig. 1a, 1,4-benzoquinone (**BQ**), capable of forming a covalent adduct with Aβ, has been demonstrated to alter the assembly routes of Aβ. These reactions, however, are initiated after Aβ accommodates certain small molecules [*e.g.*, *N*,*N*-dimethyl-*p*-phenylenediamine (**DMPD**), benzene-1,4-diamine, N^1-((1*H*-pyrrol-2-yl)methyl)-N^4,N^4-dimethylbenzene-1,4-diamine (7), and N^1,N^1-dimethyl-N^4-(thiophen-2-ylmethyl)benzene-1,4-diamine (**L1**)], which are then chemically transformed into **BQ**.[25,29–31] Moreover, **BQ** is unable to chelate metal ions, limiting its interaction with metal ions in metal–Aβ complexes. The inherent toxicity of **BQ** further restricts its biological applications.[25,32]

In this study, we illustrate an effective approach for developing novel heterocycle-fused **BQ** compounds that can control the aggregation and toxicity of both metal-free Aβ and metal–Aβ. We rationally designed and synthesized heterocycle-fused **BQ** molecules and probed their effects on the assembly and

[a]*Department of Chemistry, Korea Advanced Institute of Science and Technology (KAIST), Daejeon 34141, Republic of Korea. E-mail: miheelim@kaist.ac.kr*

[b]*Department of Applied Chemistry, Global Center for Pharmaceutical Ingredient Materials, Kyung Hee University, Gyeonggi-do 1732, Republic of Korea. E-mail: hwkim@khu.ac.kr*

† Electronic supplementary information (ESI) available: Experimental section and Fig. S1–S17. See DOI: https://doi.org/10.1039/d4sc06070a

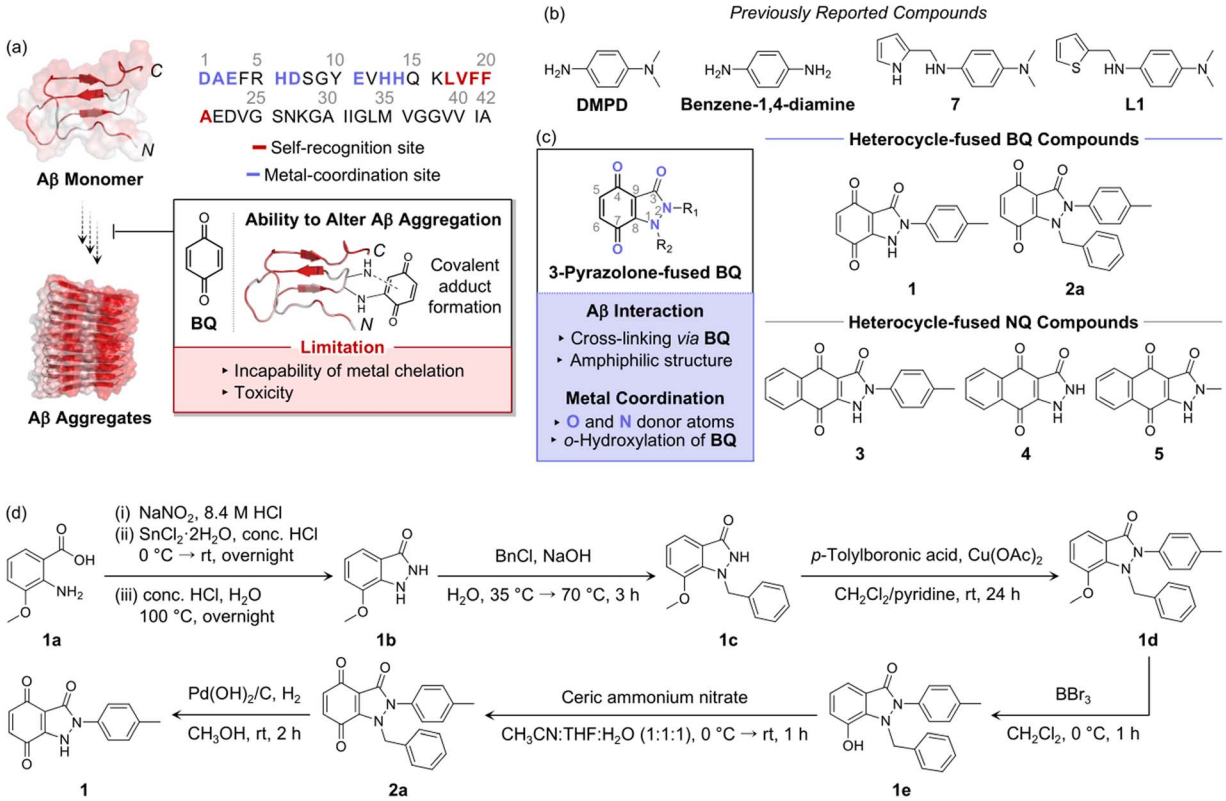

Fig. 1 Rational design and preparation of heterocycle-fused **BQ** compounds to modify the aggregation and toxicity of Aβ in the absence and presence of metal ions. (a) Ability of **BQ** to interact with Aβ and its properties that limit the reactivity of metal–Aβ and biological applications. Structures of monomeric (xx98156 [26]) and fibrillar (PDB 2BEG[27]) $Aβ_{42}$ are shown according to the Eisenberg hydrophobicity scale (hydrophilic to hydrophobic amino acid residues colored in a gradient from white to red).[28] The amino acid residues involved in the self-recognition site and metal coordination are highlighted in red and purple, respectively. (b) Previously reported compounds that can be transformed into **BQ**. (c) Chemical structures and properties of heterocycle-fused **BQ** and **NQ** compounds. **1**, 2-(*p*-Tolyl)-1*H*-indazole-3,4,7(2*H*)-trione; **2a**, 1-benzyl-2-(*p*-tolyl)-1*H*-indazole-3,4,7(2*H*)-trione; **3**, 2-(*p*-tolyl)-1*H*-benzo[*f*]indazole-3,4,9(2*H*)-trione; **4**, 1*H*-benzo[*f*]indazole-3,4,9(2*H*)-trione; **5**, 2-methyl-1*H*-benzo[*f*]indazole-3,4,9(2*H*)-trione. (d) Synthetic routes to **1** and **2a**.

toxicity of metal-free Aβ and metal–Aβ. Additionally, we determined the molecular-level mechanisms for these reactivities, including their ability to form covalent cross-links with Aβ and chelate metal ions. Our study underscores the significance of structural alterations on the **BQ** moiety for creating chemical reagents and therapeutic agents with regulatory reactivities towards metal-related peptides and proteins associated with amyloid diseases.

Results and discussion

Design principle and synthesis of compounds

For the covalent adduct formation between Aβ and the **BQ** moiety, the peptide first needs to recruit **BQ**-containing compounds. To enhance direct interactions with both metal-free Aβ and metal–Aβ, 3-pyrazolone was fused into the **BQ** moiety, as illustrated in Fig. 1b. Pyrazolones are a class of pyrazole heterocycles with various chemical and biological properties.[33–38] Particularly, the planarity of small molecules containing 3-pyrazolone combined with a benzene ring is suggested to favor the disruption of the β-sheet conformation of Aβ aggregates through hydrophobic interactions.[39] The carbonyl group on 3-pyrazolone also participates in hydrogen bonding with Aβ.[39] Furthermore, the nitrogen (N) and oxygen (O) donor atoms from the amino and carbonyl groups on 3-pyrazolone can bind to metal ions. Upon fusion with **BQ**, there are two possible metal-chelation sites: (i) a pair of N and O donor atoms from the amino and carbonyl groups at 1- and 7-positions, respectively; (ii) two O donor atoms from the carbonyl groups at 3- and 4-positions. Unlike the relatively weak metal binding of **BQ** through its carbonyl O donor atoms, metal-chelation properties of 3-pyrazolone-fused **BQ** enable a sufficient interaction with metal ions surrounded by Aβ.

Through further functionalization of the 3-pyrazolone-fused **BQ** framework, we rationally designed heterocycle-fused **BQ** compounds (**1** and **2a**; Fig. 1b). The incorporation of a *p*-tolyl group at the 2-position, without interfering with the metal-chelating moieties, generated compound **1** with increased hydrophobicity, which is suitable for hydrophobic interactions with Aβ. Previous studies have shown that a phenyl ring linked to the pyrazole moiety could engage in π–π, π–alkyl, and π–cation interactions with the Phe, Val and Leu, and Lys residues, respectively, located near and in the self-recognition site (Fig. 1a) crucial in the early stages of Aβ aggregation.[40,41]

Compound **2a**, with an additional benzyl group at the 1-position, was devised to further enhance the hydrophobicity of compound **1**, thereby improving hydrophobic contacts on Aβ and effectively controlling amyloid fibrillization. Although the benzyl group hinders the metal binding of the N donor atom at the 1-position, compound **2a** can still coordinate metal ions *via* O donor atoms from the carbonyl groups at the 3-, 4-, and 7-positions.

Since α,β-unsaturated carbonyl moieties in **BQ** are sensitive to nucleophilic attack at the β-carbon (C_β) atom, a Michael addition reaction can occur between the amino group from the side chain of Lys residues and the C_β atom at the 5- or 6-position of **BQ**, resulting in covalent cross-linking.[42] To investigate the relevance of 3-pyrazolone-fused **BQ** in modulating the reactivities with metal-free and metal-associated Aβ, we blocked the C_α and C_β atoms by fusing a benzene group, creating 3-pyrazolone-fused 1,4-naphthoquinone (**NQ**) compounds. The annulation of **BQ** in compound **1** with the benzene ring produced compound **3**, which allowed us to examine the role of the 3-pyrazolone-fused **BQ** in regulating Aβ aggregation mediated by compound **1**. Given that the presence of multiple aromatic rings in compounds enhances their ability to interact with Aβ,[22,43–49] we further designed compounds **4** and **5** to maintain the same number of aromatic rings as in compound **1** by eliminating the *p*-tolyl group at the 2-position. In the case of compound **5**, the number of donor atoms for hydrogen bonding and metal binding necessary for interacting with metal-free and metal-bound Aβ was preserved by including a methyl group at the 2-position.

As summarized in Fig. 1c, we synthesized heterocycle-fused **BQ** compounds, **1** and **2a**. Compound **1a** was diazotized to generate a diazonium salt intermediate, which was then reduced with $SnCl_2$ to synthesize a hydrazine intermediate. Intramolecular cyclization under acidic conditions produced an indazolone compound, **1b**.[50] *N*-Benzylation of **1b** with benzyl chloride under basic conditions yielded an *N*-benzylated compound, **1c**.[51] Next, **1d** was generated *via* a Cu(II)-catalyzed Chan–Evans–Lam coupling reaction of **1c** with *p*-tolylboronic acid.[52] The removal of the methyl moiety in the methoxy group of **1d** using boron tribromide (BBr_3) afforded compound **1e**.[53] Oxidation of **1e** with ceric ammonium nitrate led to the synthesis of **2a**.[54,55] Finally, compound **1** was obtained by the Pd-catalyzed hydrogenolysis of **2a** in a quantitative yield.[56,57] The synthetic routes and methods for heterocycle-fused **NQ** compounds (**3–5**) have been recently described in the patent literature.[58] The characterization of the compounds is summarized in Fig. S1–S5.†

Effects of compounds on the aggregation of metal-free Aβ and metal–Aβ

To determine the impact of our compounds on the aggregation of metal-free and metal-bound Aβ, we initially monitored the size distribution of the resultant metal-free Aβ and metal–Aβ species upon incubation with the compounds by gel electrophoresis with western blotting (gel/western blot) using an anti-Aβ antibody (6E10). In the inhibition studies presented in Fig. 2a and S6,† Aβ peptides were incubated with and without the compounds, both in the absence and presence of metal ions, to assess their effects on the formation of Aβ aggregates [Fig. 2a(i)]. As displayed in Fig. 2a(ii), heterocycle-fused **BQ** compounds, particularly **2a**, exhibited significant reactivity towards Aβ aggregation in both the absence and presence of metal ions.

Under metal-free conditions, treatment of **1** with $Aβ_{42}$ decreased the intensity of smearing at 5–11 kDa. Notably, **2a** intensified smearing across the gel lane from 5 kDa to 245 kDa. On the other hand, **3** and **4** moderately increased the band intensity at 48–135 kDa, and **5** diminished the signal intensity below *ca.* 20 kDa. In the presence of Cu(II), the intensity of bands at 35–135 kDa increased upon treatment with **1**. The Cu(II)–$Aβ_{42}$ sample treated with **2a** showed an increase in the signal intensity at 5–135 kDa. For Zn(II)–$Aβ_{42}$, the samples added with heterocycle-fused **BQ** compounds showed a clearer band at *ca.* 35 kDa relative to the compound-untreated sample, and **2a** additionally intensified the smearing at 5–20 kDa. Regarding heterocycle-fused **NQ** compounds, the band intensity for metal–$Aβ_{42}$ species at *ca.* 35 kDa was slightly enhanced by **3**. The signal at the same size was also darkened for Zn(II)–$Aβ_{42}$ treated with **4**. A significant change in the size distribution of metal–$Aβ_{42}$ was not observed with the addition of **5**. The results of the inhibition experiments with $Aβ_{40}$ also demonstrated the noticeable ability of heterocycle-fused **BQ** compounds, especially **2a**, to alter their aggregation pathways. Compound **2a** significantly changed the size distribution of metal-free $Aβ_{40}$, producing smearing between 5 kDa and 35 kDa, whereas **1** and **3–5** did not induce notable shifts in the size distribution of metal-free $Aβ_{40}$. Under Cu(II)-present conditions, new discrete bands at 5–11 kDa were detected when **1** and **2a** were incubated with $Aβ_{40}$. Conversely, **3–5** did not modify the size distribution of the aggregates. For the sample of Zn(II)–$Aβ_{40}$ incubated with **2a**, explicit bands between 5 kDa and 11 kDa were revealed, while relatively minor reactivity was observed for the samples upon addition of **1** and **3–5**, exhibiting blurred bands right above 5 kDa.

As depicted in Fig. 2a(iii), we further investigated the morphologies of the resultant Aβ aggregates by transmission electron microscopy (TEM), which can image large Aβ aggregates that have difficulty in penetrating the gel matrix.[25] Under metal-untreated conditions, all compounds fragmented long fibrils, shown in compound-free $Aβ_{42}$, into shorter filamentous species. When heterocycle-fused **BQ** compounds were incubated with Cu(II)–$Aβ_{42}$, they produced dramatically smaller aggregates with amorphous qualities compared to the compound-untreated sample, which contained larger aggregates. Treatment with **3** also reduced the size of $Aβ_{42}$ aggregates with Cu(II), but **4** and **5** did not result in considerable morphological and size changes in Cu(II)–$Aβ_{42}$ aggregates. In the presence of Zn(II), all compounds altered the morphologies of Zn(II)–$Aβ_{42}$ aggregates from fibrillary to less structured species. In particular, the **2a**-treated sample manifested chopped fibrils with small-sized amorphous aggregates. For the samples of $Aβ_{40}$, a mixture of chopped fibrils with unstructured aggregates was detected by addition of **2a** under metal-free

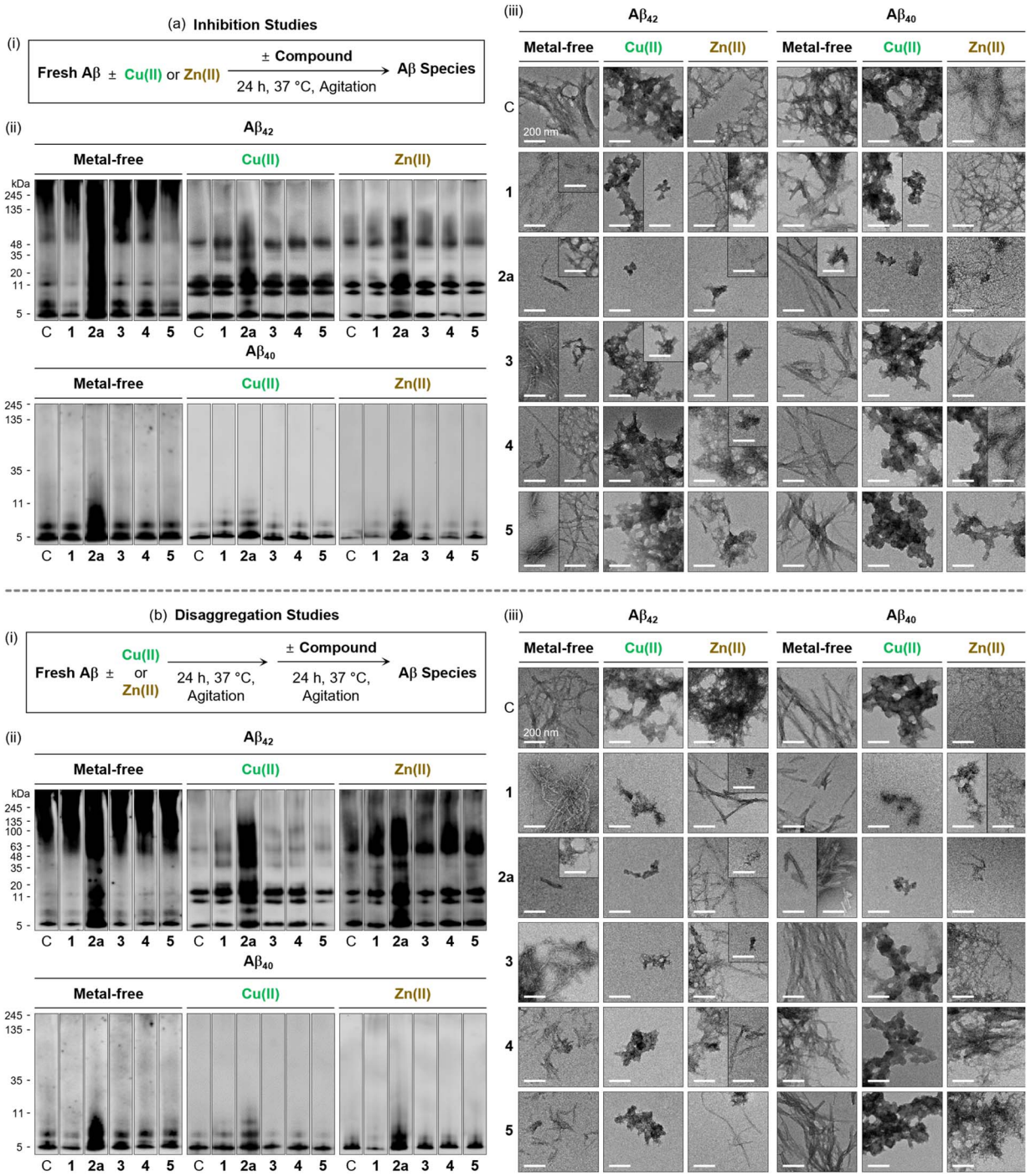

Fig. 2 Effects of compounds on the aggregation of metal-free and metal-treated Aβ analyzed by two types of experiments [(a) inhibition and (b) disaggregation studies]. (i) Scheme of Aβ aggregation experiments. (ii) Size distribution of the resultant Aβ species probed by gel/western blot using an anti-Aβ antibody (6E10). Lane C: Aβ ± Cu(II) or Zn(II). The original gel images are shown in Fig. S6.† (iii) Morphologies of the resultant Aβ species monitored by TEM. Conditions: [Aβ] = 25 μM; [Cu(II) or Zn(II)] = 25 μM; [compound] = 25 μM (1% v/v DMSO); 20 mM HEPES, pH 7.4 [for metal-free and Zn(II)-added samples] or pH 6.8 [for Cu(II)-added samples], 150 mM NaCl; 37 °C; 24 h; constant agitation. Scale bar = 200 nm.

conditions, whereas compound-free, **1**-, and **3**–**5**-treated samples showed primarily fibrillary species. In the presence of Cu(II), heterocycle-fused **BQ** compounds generated smaller amorphous aggregates compared to compound-untreated and heterocycle-fused **NQ** compound-added Cu(II)–$A\beta_{40}$. In the case of Zn(II)–$A\beta_{40}$ samples, the formation of thinner filamentous species, without and with smaller less-structured aggregates, was induced by **1** and **2a**, respectively, different from the entangled fibrillary species detected in the compound-free sample. Heterocycle-fused **NQ** compounds facilitated aggregation into less organized structures and generated chopped fibrils in **3**-incubated Zn(II)–$A\beta_{40}$. Collectively, both heterocycle-

fused **BQ** and **NQ** compounds alter the formation of Aβ aggregates to different degrees.

Moreover, the disaggregation studies were performed to identify the ability of the compounds to disassemble preformed Aβ aggregates or alter their aggregation pathways further, as illustrated in Fig. 2b and S6.† The samples were prepared by pre-incubating Aβ with and without metal ions to form preformed Aβ assembles, followed by treatment with the compounds [Fig. 2b(i)]. As shown in Fig. 2b(ii), both heterocycle-fused **BQ** and **NQ** compounds were capable of shifting the size distribution of $A\beta_{42}$ aggregates under metal-free and metal-present conditions. All compounds increased the intensity of bands at 48–63 kDa without metal ions, with **2a** prominently varying the size distribution of metal-free $A\beta_{42}$ species at 5–63 kDa. In the case of metal–$A\beta_{42}$ incubated with heterocycle-fused **BQ** compounds, the signal intensity was enhanced at 20–100 kDa and 5–135 kDa following treatment with **1** and **2a**, respectively. Heterocycle-fused **NQ** compounds slightly elevated the level of Cu(II)–$A\beta_{42}$ species at 35–100 kDa, and **5** also decreased the signal at 5–11 kDa. In the presence of Zn(II), the size distribution of $A\beta_{42}$ at 63–135 kDa was shifted by **3–5**. For the experiments with $A\beta_{40}$, incubation of heterocycle-fused **BQ** compounds remarkably altered the amount of $A\beta_{40}$ oligomers between 5 kDa and 11 kDa under both metal-free and metal-present conditions, compared to the samples without compounds and those treated with heterocycle-fused **NQ** compounds, which showed less reactivity.

In the TEM studies depicted in Fig. 2b(iii), **1** and **3** produced thinner metal-free $A\beta_{42}$ fibrils, compared to relatively thicker and longer fibrillary aggregates observed in the compound-free sample, while **2a**, **4**, and **5** shortened the fibrils. The size of Cu(II)–$A\beta_{42}$ aggregates was dramatically reduced by addition of both heterocycle-fused **BQ** and **NQ** compounds. Under Zn(II)-treated conditions, all compounds generated thinner filamentous species different from the bundle of fibrillar aggregates of compound-free Zn(II)–$A\beta_{42}$, and smaller amorphous aggregates were also shown for the samples incubated with **1**, **2a**, and **3**. For $A\beta_{40}$, both **1** and **2a** remarkably truncated fibrillary species displayed in the compound-free sample under metal-free conditions. In the presence of Cu(II), the addition of heterocycle-fused **BQ** compounds induced the formation of smaller-sized amorphous aggregates. Under Zn(II)-present conditions, relative to Zn(II)–$A\beta_{40}$ aggregates with fibrillary characteristics, a mixture of amorphous and fibrillary aggregates was monitored upon treatment of **1** with $A\beta_{40}$ aggregates, and the addition of **2a** triggered the formation of chopped fibrils. In contrast, little or no morphological alteration was detected for the samples prepared with heterocycle-fused **NQ** compounds. Overall, both heterocycle-fused **BQ** and **NQ** compounds can disassemble the preformed Aβ aggregates or additionally alter their aggregation pathways in the absence and presence of metal ions to distinct extents. Heterocycle-fused **BQ** compounds exhibited significant modulatory effects on the aggregation of metal-free and metal-associated Aβ over heterocycle-fused **NQ** compounds. This indicates that the structural modifications on the **BQ** moiety, without the fusion of an additional benzene ring at the 5- and 6-positions, are essential for impacting the assembly of Aβ with and without metal ions. Notably, the enhanced ability of **2a** relative to **1** in changing the size distribution and morphology of Aβ aggregates under both metal-free and metal-treated conditions suggests that the benzyl ring at the 1-position of **2a** contributes to its regulatory reactivity with metal-free Aβ and metal–Aβ.

Mechanistic studies (I): interactions of compounds with metal-free Aβ

To elucidate the distinct reactivities of heterocycle-fused **BQ** and **NQ** compounds towards Aβ aggregation, we investigated their interactions with Aβ peptides. Considering that $A\beta_{42}$ is more pathogenic than $A\beta_{40}$,[59] and the modulative effects of our compounds were more discernible in the samples with $A\beta_{42}$ rather than $A\beta_{40}$ (Fig. 2), we focused on analyzing the direct interactions between the compounds and $A\beta_{42}$ by electrospray ionization–mass spectrometry (ESI–MS). As presented in Fig. 3a, metal-free $A\beta_{42}$ incubated with **1** and **3–5** showed the peaks assigned to non-covalent adducts of $A\beta_{42}$ with the compounds at 1589 *m*/*z*, 1606 *m*/*z*, 1576 *m*/*z*, and 1580 *m*/*z*, respectively. In the presence of **2a** (344 Da), a peak corresponding to the addition of 342 Da to the 3+-charged $A\beta_{42}$ monomer (4511 Da) was detected at 1619 *m*/*z*, likely representing the covalent adduct of **2a** with metal-free $A\beta_{42}$. Further fragmental analysis of the peak through collision-induced dissociation (CID) identified the amino acid residue in $A\beta_{42}$ involved in the formation of this covalent cross-linking. In tandem MS (ESI–MS^2) depicted in Fig. 3b, *b* fragments smaller than b_{16} were observed in their native forms. Starting from b_{16}, the *b* fragments were detected with and without the addition of 342 Da, suggesting Lys16 as the amino acid residue forming a covalent bond with **2a**. Native forms of *b* fragments were no longer monitored beyond b_{27}, indicating that Lys28 could also be a site for covalent cross-linking with **2a**.

Lys residues in several amyloidogenic peptides and proteins have been reported to facilitate both hydrophobic and electrostatic interactions *via* flexible butyl and ε-ammonium groups in their side chains, respectively, in the intramolecular and intermolecular manner.[60,61] More specifically, Lys16, adjacent to the self-recognition site (Fig. 1a), forms a salt bridge with Glu22 in the fibril structure of Aβ[62] or is exposed to the solvent, making it available for interacting with other monomers.[63] Additionally, Lys28 stabilizes the turn structure of monomeric Aβ through a salt bridge with Asp23, which can mediate the folding and assembly of Aβ.[62,64–66] Therefore, the covalent bond formation between the **BQ** moiety in **2a** and Lys residues of $A\beta_{42}$ could be critical in altering its aggregation pathways.

Interestingly, this phenomenon was observed only in the sample incubated with **2a**, not with **1**. This implies the involvement of the benzyl ring at the 1-position of **2a** in the covalent adduct formation with $A\beta_{42}$. Based on the potential interactions between **2a** and monomeric $A\beta_{42}$ visualized by docking studies (Fig. 3c), the benzyl group can participate in CH–π interactions with Lys16 and Phe20. This suggests that this benzyl functionality may facilitate the recruitment of **2a** by $A\beta_{42}$, followed by the cross-linking reaction between them.

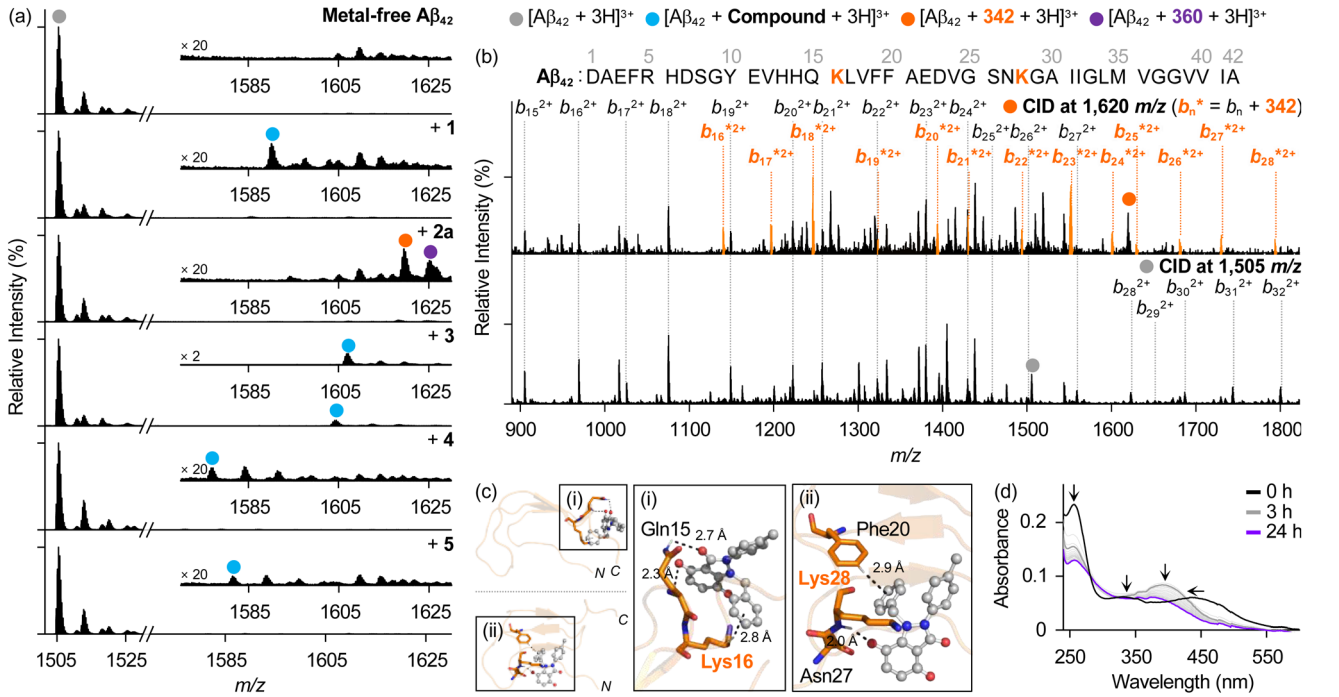

Fig. 3 Interaction of compounds with metal-free $A\beta_{42}$ and **2a**'s chemical transformation. (a) ESI–MS studies of metal-free $A\beta_{42}$ with and without compounds. Conditions: $[A\beta_{42}]$ = 25 μM; [compound] = 25 μM (1% v/v DMSO); 20 mM ammonium acetate, pH 7.4; 37 °C; 24 h; constant agitation. The samples were diluted 25-fold with H_2O before injection into the mass spectrometer. (b) ESI–MS^2 investigations of metal-free $A\beta_{42}$ with (top; 1620 *m*/*z*) and without (bottom; 1505 *m*/*z*) covalent bond formation with **2a**. (c) Possible interactions of **2a** with metal-free $A\beta_{42}$ (xx98156 (ref. 26)) visualized by docking studies. Nine docked models were obtained with binding energies ranging from −5.9 to −5.5 kcal mol^{-1}, and two representative models are indicated in (i) and (ii). (d) Chemical transformation of **2a** monitored by Abs spectroscopy. Conditions: [**2a**] = 25 μM (1% v/v DMSO); 20 mM HEPES, pH 7.4, 150 mM NaCl; 37 °C; 24 h; no agitation.

Furthermore, **2a** is positioned near the self-recognition and C-terminal regions, encompassing the Lys16 and Lys28 residues as Michael donors for forming covalent bonds with **2a**. Multiple hydrogen bonds were also predicted for the carbonyl O atoms located at the 3-, 4-, and 7-positions of **2a** with the amide group from the side chain of Gln15 and the backbone amide moieties between Gln15 and Lys16, and Asn27 and Lys28.

Moreover, an additional peak at 1624 *m*/*z*, indicating a mass shift of +360 Da from metal-free $A\beta_{42}$ monomer, appeared upon incubation with **2a**. The nature of this peak was first analyzed by examining the chemical transformation of **2a** by electronic absorption (Abs) spectroscopy, as shown in Fig. 3d. The optical spectrum of **2a** in aqueous solution exhibited three Abs bands at *ca*. 255 nm, 330 nm, and 440 nm, consistent with those observed for **BQ**.[67–69] After 24 h of incubation, the spectral features at the shortest wavelength diminished, while a hypsochromic shift from *ca*. 440 nm to *ca*. 390 nm and a bathochromic shift from *ca*. 255 nm to *ca*. 265 nm were monitored, indicative of *o*-hydroxylation of the **BQ** moiety in **2a**.[67–69] Previous studies have proposed that the reaction of **BQ** with H_2O at neutral pH triggers the formation of enolized **BQ** [4,6-dihydroxycyclohexa-2,4-dien-1-one; **BQ(H_2O)**], which can be rearranged into 1,2,4-trihydroxybenzene (**THB**) (Fig. S7a†).[67–69] Oxidation of **BQ(H_2O)** by **BQ** and auto-oxidation of **THB** subsequently produce **2-hydroxy-BQ** (2-hydroxycyclohexa-2,5-diene-1,4-dione).[67–69] As depicted in Fig. S8,† the mass spectrum of **2a** incubated for 24 h in aqueous solution displayed a peak assigned to $[\mathbf{2a} + 16 + H]^+$, plausibly denoting **2a** substituted with a hydroxyl group (**2b**; *vide infra*). Thus, the peak at 1624 *m*/*z* in the mass spectrum of **2a**-treated metal-free $A\beta_{42}$ (Fig. 3a) can arise from the non-covalent adduct formation between monomeric $A\beta_{42}$ and **2a** containing a hydroxylated **BQ** moiety.

In summary, both heterocycle-fused **BQ** and **NQ** compounds can directly interact with monomeric $A\beta_{42}$. We further confirmed that **2a**, compared to **1**, can participate in the generation of covalent bonds with $A\beta_{42}$. These suggest that a supplementary benzyl moiety at the 1-position of **2a** is required for sufficient contact with Aβ, consequently producing a covalent cross-link to the peptide *via* **BQ**. Moreover, **2a** undergoes *o*-hydroxylation of the **BQ** moiety and, subsequently, directly interacts with Aβ. Such **2a**-driven interactions with metal-free Aβ support its significant reactivity towards Aβ in both the absence and presence of metal ions.

Mechanistic studies (II): interactions of chemically transformed 2a with metal ions, metal-free Aβ, and metal–Aβ

To gain a better understanding of the involvement of chemically transformed **2a** in its reactivity towards the aggregation of metal-free Aβ and metal–Aβ, we synthesized compound **2b**, which is **2a** with a hydroxyl group at the 6-position, and analyzed its interactions with metal ions, metal-free Aβ, and metal–Aβ. As presented in Fig. 4a, compound **1e** was dibrominated with Br_2, yielding 4,6-dibromo-indazolone and the

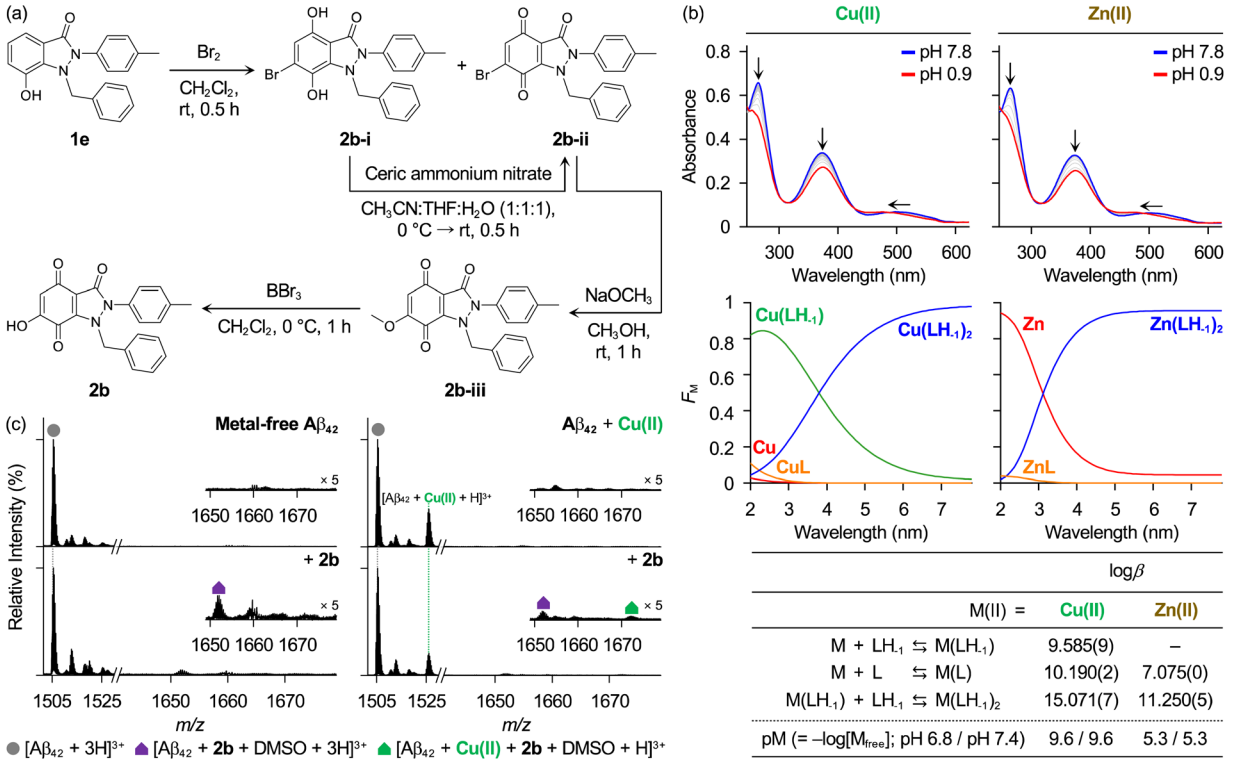

Fig. 4 Preparation of **2b** and its ability to interact with metal ions, metal-free Aβ$_{42}$, and Cu(II)–Aβ$_{42}$. (a) Synthetic routes to **2b** [1-benzyl-6-hydroxy-2-(*p*-tolyl)-1*H*-indazole-3,4,7(2*H*)-trione]. (b) Solution speciation studies of metal–**2b** (L) complexes. Abs variable-pH titration spectra (top) and the solution speciation diagram (middle) were obtained by titrations of metal–ligand complexes (F_M = fraction of species at a given pH). The log β and pM values of metal–ligand complexes are summarized in the table (bottom). The errors in the last digit are shown in parentheses. Charges are omitted for clarity. Conditions: [**2b**] = 50 μM; [Cu(II) or Zn(II)] = 25 μM; room temperature; I = 0.1 M NaCl. (c) Interactions of **2b** with metal-free Aβ$_{42}$ and Cu(II)–Aβ$_{42}$ monitored by ESI–MS. Conditions: [Aβ$_{42}$] = 25 μM; [Cu(II)] = 25 μM; [**2b**] = 25 μM (1% v/v DMSO); 20 mM ammonium acetate, pH 7.4 (for metal-free samples) or pH 6.8 [for Cu(II)-treated samples]; 37 °C; 24 h; constant agitation. The samples were diluted 25-fold with H_2O before injection into the mass spectrometer.

unexpected 6-bromo-benzoquinone (**6-Br-BQ**) derivative.[70] We assumed that the latter was oxidized by H_2O and Br_2 derived from 4,6-dibromo-indazolone. Consequently, the reaction conditions were established to synthesize 6-bromo-4,7-dihydroxyindazolone, **2b-i**, and **6-Br-BQ** derivative, **2b-ii**. **2b-i** was oxidized to **2b-ii** using ceric ammonium nitrate.[54,55] The subsequent methoxylation of **2b-ii** with sodium methoxide ($NaOCH_3$) resulted in the formation of a 6-methoxy-benzoquinone derivative, **2b-iii**.[71] Finally, **2b** was obtained by the demethylation of **2b-iii** using BBr_3 in a high yield.[72] The characterization of **2b** is summarized in Fig. S9.† It is noteworthy that spectral features of **2b** in aqueous solution are similar to those of **2a** incubated for 24 h, but with greater optical intensity. This observation supports that **2a** undergoes chemical transformations into **2b** and various other products, including less soluble aggregates (*vide infra*).[67–69,73–75]

o-Hydroxylation of **BQ** in **2a** introduces an additional metal-chelation site, composed of a pair of O donor atoms from hydroxyl and carbonyl groups at the 6- and 7-positions, respectively. To explore the capacity of **2b** to bind metal ions in aqueous solution, solution speciation studies with Abs variable-pH titrations were performed. Initially, the solution of **2b** (L) was titrated with small aliquots of HCl under metal-free conditions to estimate its acidity constants (K_a). As illustrated in Fig. S10,† two pK_a values, 0.627(5) and 4.827(5), were calculated. The solution speciation diagram displayed the presence of anionic (LH_{-1}), neutral (L), and monoprotonated (LH) forms of **2b** in the pH range from 2 to 9. The anionic form of the ligand was predicted to predominate at pH 6.8, a condition representing a physiologically acidotic environment where Aβ assembly can be accelerated in the presence of Cu(II),[76] and at physiological pH 7.4, accounting for *ca.* 98% and *ca.* 100% relative abundance, respectively.

Subsequently, solution speciation experiments of **2b** were conducted in the presence of Cu(II) and Zn(II) to identify the metal-to-ligand stoichiometry and ligand's metal-binding affinities. As shown in Fig. 4b, the stability constants (β) were calculated for the formation of metal–**2b** complexes plausibly present at pH 0.9–7.8. Metal complexes with the 1 : 2 metal-to-ligand stoichiometry were indicated as a major species at pH 6.8 and pH 7.4. Based on the protonation and metal complexation of **2b** at the given pH and concentrations of the ligand and metal ions, the values of pM ($-\log[M_{free}]$, where $[M_{free}]$ denotes the concentration of unchelated metal ions) were computed to predict the relative metal-binding ability of **2b** under our experimental conditions.[77,78] At pH 6.8 and pH 7.4, **2b** presented

pCu and pZn values of 7.7 and 5.3, respectively. It should be noted that the metal-binding affinity of **2a** could not be experimentally determined due to its chemical transformation in aqueous solution. Instead, we evaluated the metal-binding ability of **6** which is derivatized from **3**, which features the substitution of the amino group at the 1-position with a methyl group and the replacement of the *p*-tolyl group at the 2-position with a phenyl ring.[58,79] This compound is relatively stable under our experimental conditions and has potential for metal chelation through two carbonyl O donor atoms in the 3- and 4-positions, similar to **2a**; however, no significant spectral change was detected in Abs spectra of the compound upon addition of Cu(II) (Fig. S11†). This corroborates the limited capability of **2a** to interact with metal ions under our experimental settings. These results underline that the chemical transformation of **2a** imparts the ability to chelate metal ions (Fig. 1b).

To verify the interaction between **2b** and $A\beta_{42}$ with and without metal ions, ESI–MS studies were carried out. As depicted in Fig. 4c and S12,† new peaks at 1651 *m*/*z* were detected upon addition of **2b** to $A\beta_{42}$ under both metal-free and metal-present conditions, assigned to $[A\beta_{42} + \mathbf{2b} + DMSO + 3H]^{3+}$. In the presence of Cu(II), a peak at 1671 *m*/*z* corresponding to $[A\beta_{42} + Cu(II) + \mathbf{2b} + DMSO + H]^{3+}$ was observed, indicating the formation of a ternary complex composed of $A\beta_{42}$, Cu(II), and **2b**. This compound also generated a ternary complex with Zn(II)–$A\beta_{42}$ (Fig. S12†). The pM values of **2b** (Fig. 4b), comparable to those of Aβ (*ca.* 6–12 for pCu at pH 6.5–7.4; *ca.* 6 for pZn at pH 7.4),[11,13,80,81] support such competitive metal coordination of **2b** with Aβ. These findings demonstrate that **2b** can interact with metal ions as well as Aβ in both the absence and presence of metal ions. Consequently, the chemical transformation of **2a**, including *o*-hydroxylation likely into **2b**, enables it to chelate metal ions in a bidentate manner with binding affinities similar to those of Aβ, ultimately impacting the self-assembly of metal–Aβ.

Mechanistic studies (III): impact of 2b on the aggregation of metal-free Aβ and metal–Aβ

The effect of **2b** on the assembly of metal-free Aβ and metal–Aβ was further probed by gel/western blot using 6E10 and TEM. In the inhibition studies, the size distribution of Aβ species with and without metal ions was not significantly influenced by **2b**, as delineated in Fig. 5a and S6;† however, the impact of **2b** on the aggregation of the peptides in the absence and presence of metal ions was discernibly shown in the TEM studies. The resultant $A\beta_{42}$ and $A\beta_{40}$ aggregates produced in the presence of **2b** were analyzed as shorter fibrils relative to compound-free samples, which showed significant fibrillar aggregates under metal-free and Zn(II)-added conditions, as illustrated in Fig. 5b. Upon incubation of **2b** with Cu(II)–Aβ, a mixture of smaller aggregates with amorphous and fibrillary characteristics was generated for $A\beta_{42}$ and $A\beta_{40}$, differing from compound-free samples, which mainly displayed larger aggregates. Together, **2b** and **2a** affect the formation of Aβ aggregates in the absence and presence of metal ions to distinct extents.

In the disaggregation studies conducted by gel/western blot using 6E10, as shown in Fig. S6 and S13,† the reactivity of **2b**

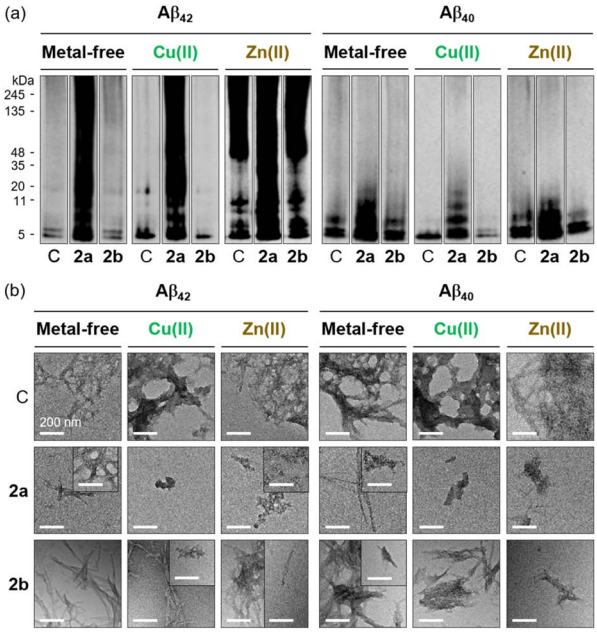

Fig. 5 Impact of **2a** and **2b** on the formation of metal-free and metal-associated Aβ aggregates. (a) Size distribution of the resultant Aβ species analyzed by gel/western blot using 6E10. Lane C: Aβ ± Cu(II) or Zn(II). The original gel images are shown in Fig. S6.† (b) Morphologies of the resultant Aβ species investigated by TEM. Conditions: [Aβ] = 25 μM; [Cu(II) or Zn(II)] = 25 μM; [compound] = 25 μM (1% v/v DMSO); 20 mM HEPES, pH 7.4 [for metal-free and Zn(II)-containing samples] or pH 6.8 [for Cu(II)-containing samples], 150 mM NaCl; 37 °C; 24 h; constant agitation. Scale bar = 200 nm.

with metal-free and metal-associated Aβ was not clearly monitored. TEM, however, presented that **2b**-added $A\beta_{42}$ and $A\beta_{40}$ samples included shorter and chopped fibrils, different from compound-unadded samples which exhibited bigger aggregates, under metal-free and metal-added conditions. These findings indicate that both **2b** and **2a** can disassemble preformed Aβ aggregates or additionally alter their aggregation profiles in the absence and presence of metal ions to varying degrees. Overall, **2b**, as the chemically transformed form of **2a**, can modulate the aggregation pathways of Aβ in both the absence and presence of metal ions, potentially contributing to the reactivity of **2a** with metal-free Aβ and metal–Aβ. Given that Aβ samples incubated with **2a** contain various chemically transformed forms of **2a**, the reactivity of **2a** towards Aβ aggregation with and without metal ions may be influenced not only by **2b** but also by other chemically transformed forms, as well as intact **2a** (Fig. S7b†). It should be noted that we monitored the formation of **2b′** upon incubation of **2a** for 6 h in aqueous media, followed by its disappearance after 24 h, as depicted in Fig. S8.† According to previous studies, compounds with multiple aromatic rings can participate in π–π stacking, leading to the generation of relatively less soluble aggregates that become optically undetectable.[71,72] The aggregates present in **2a**- and **2b**-incubated samples, which differ in composition and relative abundance, may further influence the extent to which **2a** and **2b** affect the assembly of Aβ. In addition, as shown in

Fig. S7c,† a hydroxyl group at the 6-position of **2b** enables additional hydrogen bonding with Aβ, potentially altering its reactivity with Aβ in the absence and presence of metal ions compared to **2a**.

Mechanistic studies (IV): metal-binding properties of compounds and modifications of Aβ by compounds in the presence of Cu(II)

Apart from **2a**, **1** and **3–5** share two possible metal-chelation sites: N and O donor atoms at the 1- and 7-positions, respectively, and two O donor atoms at the 3- and 4-positions. Given that their metal-binding ability can mediate their reactivity with metal–Aβ, metal-binding properties of **1** as a representative molecule were analyzed. Job's method of continuous variation was used to determine the Cu(II)-to-ligand stoichiometry (Fig. S14a†). We mixed **1** and Cu(II) at various ratios while maintaining their total concentration and traced the Abs at 250 nm. The Job plot revealed a maximum intensity at a mole fraction of Cu(II) of *ca.* 0.3 with an asymmetrical curve shape, suggesting that a mixture of Cu(II)–**1** complexes with 1 : 1 and 1 : 2 Cu(II)-to-ligand ratios could exist in aqueous solution.[82,83] Next, we titrated the aqueous solution of **1** with Cu(II) and monitored the spectral changes at 250 nm (Fig. S14b and c†). These led to estimating the dissociation constants (K_d) of **1** for Cu(II) to be in the micromolar range. Although this Cu(II)-binding affinity is likely insufficient to effectively interact with the primary Cu(II)-binding site in Aβ, which has a nanomolar affinity, the presence of a second Cu(II)-binding site, with an affinity in the micromolar range,[10,30,84] implies that the interaction of **1** and **3–5** with Cu(II) at this secondary site in Aβ may still be feasible. It should be noted that the pK_a value of **1** and its Zn(II)-binding affinity could not be determined due to the limited spectral change within the pH range monitored for our measurements without dilution effects and upon incubation with Zn(II), respectively, under our experimental conditions (Fig. S15†).

We then examined the samples of metal–Aβ_{42} incubated with heterocycle-fused **BQ** or **NQ** compounds by ESI–MS. As presented in Fig. 6a, **1** and **3–5** formed non-covalent adducts with Aβ_{42} in the presence of Cu(II), similar to what was observed under metal-free conditions (1589 *m*/*z*, 1606 *m*/*z*, 1576 *m*/*z*, and 1580 *m*/*z* for **1**, **3**, **4**, and **5**, respectively). **3** additionally indicated the ternary complexation with Aβ_{42} and Cu(II) (1626 *m*/*z*). Under Zn(II)-present conditions, all compounds could also interact with Aβ_{42} similar to their behavior in the absence of metal ions

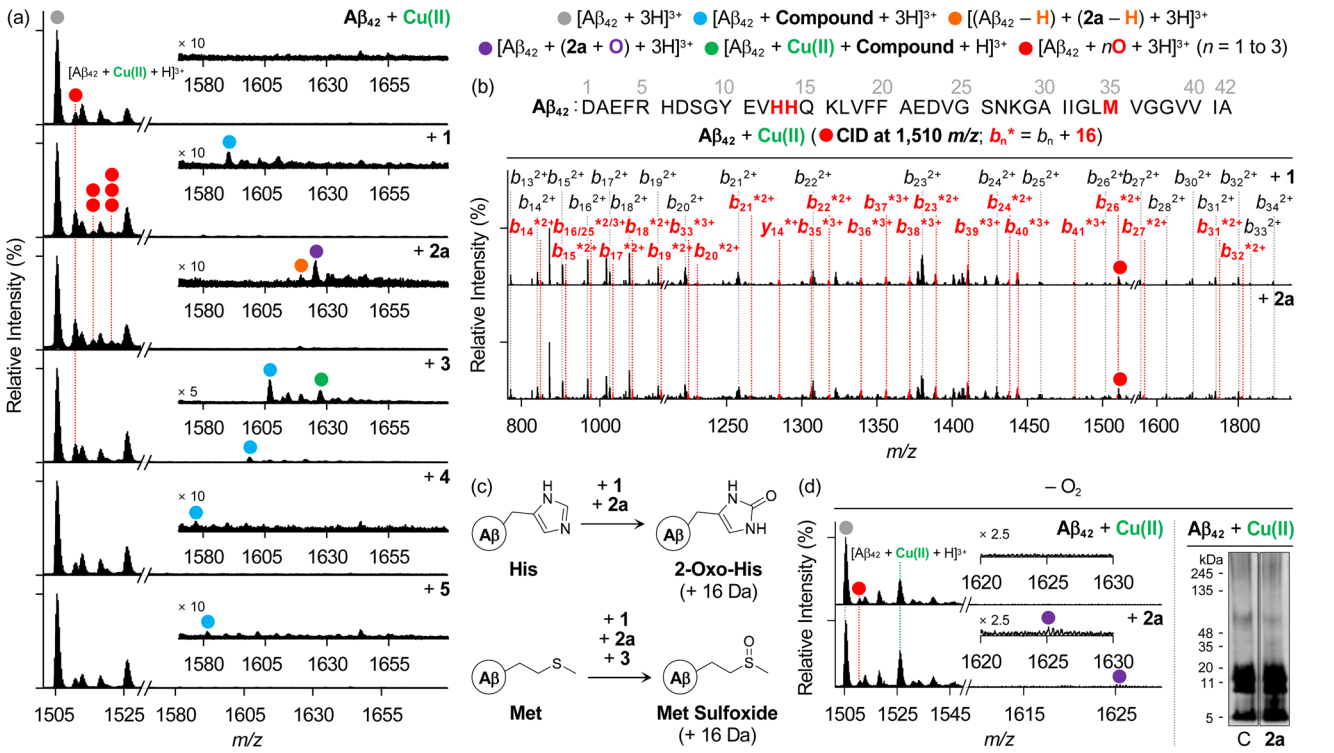

Fig. 6 Analysis of Cu(II)–Aβ_{42} upon addition of compounds in the absence and presence of O_2. (a) ESI–MS studies of Cu(II)-added Aβ_{42} samples with and without compounds under aerobic conditions. The number of red circles represents that of O atoms incorporated into the Aβ_{42} monomer. Conditions: [Aβ_{42}] = 25 μM; [Cu(II)] = 25 μM; [compound] = 25 μM (1% v/v DMSO); 20 mM ammonium acetate, pH 6.8; 37 °C; 24 h; constant agitation. The samples were diluted 25-fold with H_2O before injection into the mass spectrometer. (b) ESI–MS^2 analysis of the singly oxidized Aβ_{42} obtained by incubation with heterocycle-fused **BQ** compounds. (c) Oxidation of His and Met residues observed in this work. (d) Analysis of Cu(II)–Aβ_{42} samples upon incubation with **2a** under anaerobic conditions by ESI–MS (left) and gel/western blot using 6E10 (right). Lanes: (C) Aβ + Cu(II); (2a) C + **2a**. The original gel images are shown in Fig. S6.† Conditions: [Aβ_{42}] = 25 μM; [Cu(II)] = 25 μM; [**2a**] = 25 μM (1% v/v DMSO); 20 mM ammonium acetate, pH 6.8 (for ESI–MS) or 20 mM HEPES, pH 6.8, 150 mM NaCl (for gel/western blot); 37 °C; 24 h; quiescent conditions. The samples were diluted 25-fold with H_2O before injection into the mass spectrometer.

(Fig. S16†). Interestingly, consecutive peaks appeared in the Cu(II)–Aβ_{42} samples added with heterocycle-fused **BQ** compounds at 1510 *m*/*z*, 1515 *m*/*z*, and 1520 *m*/*z*, corresponding to singly, doubly, and triply oxidized Aβ_{42}, respectively. Upon applying the CID energy to the peak at 1510 *m*/*z*, as depicted in Fig. 6b, *b* fragments from b_{13} were exhibited in their non-oxidized and oxidized forms, indicating that heterocycle-fused **BQ** compounds oxidized His13, His14, or Met35. The CID of the peaks assigned to doubly and triply oxidized peptides could not be well-resolved under our experimental settings, but three plausible oxidation sites imply that heterocycle-fused **BQ** compounds simultaneously oxidize two or three of His13, His14, and Met35.

As summarized in Fig. 6c, the structural conversion of His into 2-oxo-His, caused by heterocycle-fused **BQ** compounds, was reported to change the polarity of His, leading to disturbances in electrostatic interactions of Aβ peptides, thereby modifying their assembly profiles.[12,85] Additionally, His residues are included in the metal-coordination site in Aβ (Fig. 1a) and, thus, their structural modification affects metal binding to Aβ peptides and their aggregation pathways in the presence of metal ions.[11] Furthermore, the oxidative modification of the Met residue results in Met sulfoxide, which can alter the secondary structures across the peptides, reducing their hydrophobic and electrostatic associations.[86–89] In the case of the **3**-treated sample, a singly oxidized Aβ_{42} monomer was also shown (Fig. 6a), and Met35 was revealed to be the oxidation site, as detected for the compound-free Cu(II)–Aβ_{42} sample (Fig. S17†).

To verify the involvement of copper–O_2 chemistry in the oxidative transformation of Aβ,[90,91] the samples of Cu(II)–Aβ_{42} incubated with and without **2a** under anaerobic conditions were further explored, as shown in Fig. 6d. Distinct from the mass spectra obtained under aerobic conditions (Fig. 6a), there was no notable variation in the signal intensity of the singly oxidized Aβ_{42} monomer upon treatment with **2a**, and the peaks assigned to multiply oxidized peptides were not observed in the absence of O_2. Thus, copper–O_2 chemistry may promote the oxidative modifications of Aβ in the presence of **2a**. Notably, Aβ_{42} still formed a non-covalent adduct with the chemically transformed **2a** (**2a** containing *o*-hydroxylated **BQ**) under anaerobic conditions. In the gel/western blot using 6E10, **2a** produced Aβ oligomers of 5–11 kDa. According to the ESI–MS results, Cu(II)-added Aβ_{42} aggregation could be varied even without O_2 by the chemical transformation of **2a** and its subsequent interaction with Aβ_{42}. Our biophysical and biochemical observations substantiate the direct interactions of both heterocycle-fused **BQ** and **NQ** compounds with Aβ in the presence of metal ions. Heterocycle-fused **BQ** compounds, particularly **2a**, can concurrently oxidize multiple amino acid residues in Aβ in the presence of Cu(II) depending on the availability of O_2, changing the aggregation patterns of Cu(II)–Aβ with and without O_2 in a distinct manner.

Cytotoxicity of compounds and their influence on Aβ-induced cytotoxicity with and without metal ions

As our compounds affect the aggregation pathways of Aβ in the absence and presence of metal ions (Fig. 2, 5 and S13†), their ability to control the cytotoxicity induced by Aβ with and without metal ions was assessed by the MTT assay [MTT = 3-(4,5-dimethylthiazol-2-yl)-2,5-diphenyltetrazolium bromide] employing human neuroblastoma SH-SY5Y (5Y) cells (Fig. 7a). Prior to conducting cell studies with Aβ, the cytotoxicity of heterocycle-fused **BQ** and **NQ** compounds and **2b** was evaluated under metal-free and metal-present conditions and compared

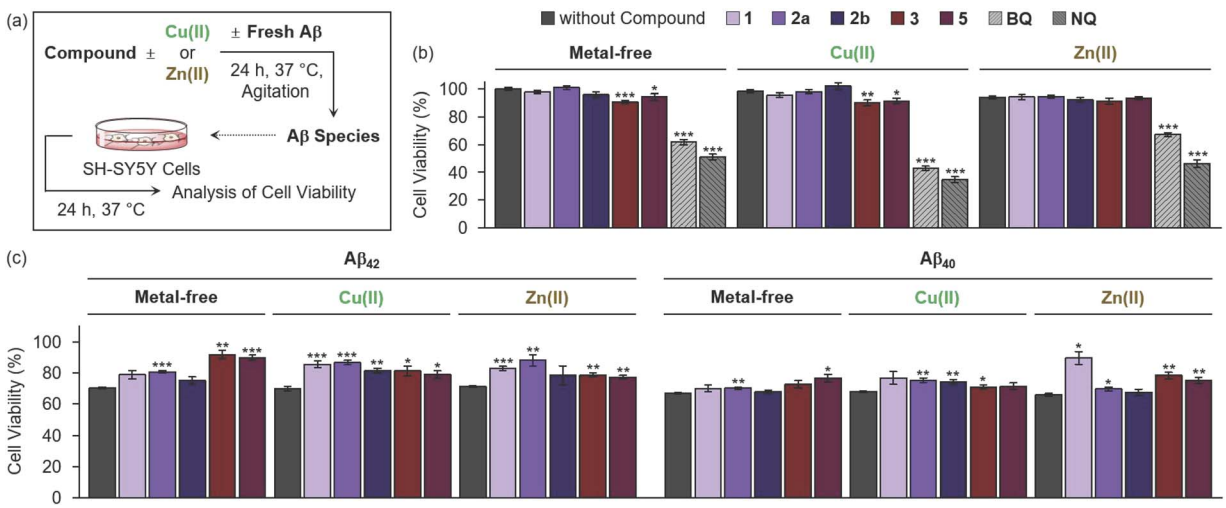

Fig. 7 Cytotoxicity of compounds under metal-free and metal-treated conditions and their impact on the cytotoxicity induced by metal-free and metal-associated Aβ. (a) Scheme of the experiments. (b) Viability (%) of 5Y cells upon incubation with heterocycle-fused **BQ** or **NQ** compounds, **2b**, **BQ**, or **NQ** with and without metal ions. (c) Influence of heterocycle-fused **BQ** and **NQ** compounds and **2b** on the cytotoxicity mediated by metal-free and metal-treated Aβ. The MTT assay provided the cell survival (%), calculated relative to that of cells treated with an equivalent amount of the buffered solution (20 mM HEPES, pH 7.4 or pH 6.8, 150 mM NaCl) with 0.2% v/v DMSO. Conditions: [Aβ] = 25 μM; [Cu(II) or Zn(II)] = 25 μM; [compound] = 25 μM (0.2% v/v DMSO); 20 mM HEPES, pH 7.4 [for metal-free and Zn(II)-added samples] or pH 6.8 [for Cu(II)-added samples], 150 mM NaCl. All values are indicated as mean ± SEM. Statistically significant difference from compound-untreated controls was determined by a two-sided unpaired Student's *t*-test (*$P < 0.05$, **$P < 0.01$, or ***$P < 0.001$).

with that of **BQ** and **NQ**. As shown in Fig. 7b, no significant cytotoxicity was observed for heterocycle-fused **BQ** and **NQ** compounds and **2b** in both the absence and presence of metal ions (cell survival over 90%) at the concentrations used for cell studies with Aβ. In contrast, **BQ** and **NQ** severely decreased cell survival by *ca*. 33–65% regardless of the presence of metal ions. These results demonstrate that the fusion of **BQ** and **NQ** on the 3-pyrazole framework, with and without the substitution at the 1- or 2-position or both, as well as the 6-position, can mitigate their cytotoxicity. It should be noted that the cytotoxicity of **4** could not be determined due to its limited solubility under our experimental conditions.

Moving forward, Aβ species preincubated with and without heterocycle-fused **BQ** or **NQ** compounds in the absence and presence of metal ions were introduced into the cells. As illustrated in Fig. 7c, some compounds exhibited substantial mitigating effects on the cytotoxicity triggered by Aβ with and without metal ions. The amelioration of metal-free $A\beta_{42}$-induced cytotoxicity was achieved by addition of **2a**, enhancing cell viability by *ca*. 10%. When **1** and **2a** were incubated with metal–$A\beta_{42}$, the cell survival increased by *ca*. 12–17%. Treatment of **2b** decreased the cytotoxicity of Cu(II)–$A\beta_{42}$ by *ca*. 12%. Cells added with metal-free and metal-associated $A\beta_{42}$ with heterocycle-fused **NQ** compounds also showed an increase in cell viability by *ca*. 6–22%, compared to those treated with compound-free samples. In the case of $A\beta_{40}$, the cell survival was enhanced upon treatment with **1** in the presence of Zn(II) and **2a** with and without metal ions by *ca*. 23% and *ca*. 3–7%, respectively. The addition of **2b** with Cu(II)–$A\beta_{40}$ improved cell viability by *ca*. 6%. Regarding heterocycle-fused **NQ** compounds, **3** lowered metal–$A\beta_{40}$-induced cytotoxicity by *ca*. 3–12%, and **5** also reduced cellular death mediated by $A\beta_{40}$ under metal-free and Zn(II)-present conditions by *ca*. 9–10%. Overall, our investigations confirm that heterocycle-fused **BQ** and **NQ** compounds and **2b** exert cytoprotective effects against metal-free and metal-associated Aβ.

Conclusions

AD is linked to the self-assembly of Aβ in the absence and presence of metal ions, resulting in neurotoxic aggregates observed as deposits in the patients' brains.[10–14,19,21,92] In an effort to modulate the aggregation of Aβ, small molecules that can be converted into **BQ** have been reported.[25,29,30,73] Following their chemical transformation, **BQ** forms covalent adducts with Aβ peptides, with a consequent impact on their assembly routes;[25,29,30] however, the inability to chelate metal ions and the significant toxicity of **BQ** have limited its reactivity with metal–Aβ and its biological applications. In this work, we demonstrate how to effectively design heterocycle-fused **BQ** compounds that modulate the aggregation of both metal-free Aβ and metal–Aβ by leveraging the strength of **BQ** (*e.g.*, covalent cross-linking to Aβ) while addressing its weaknesses (*e.g.*, poor metal chelation and toxicity).

We rationally designed bidentate ligands by combining **BQ** with the 3-pyrazolone framework, varying the type, position, and number of substituents on the 3-pyrazolone group without (**1** and **2a**) and with (**3–5**) the annulation of **BQ** with a benzene ring. Our multidisciplinary investigations reveal that heterocycle-fused **BQ** compounds significantly regulate the aggregation of metal-free Aβ and metal–Aβ, while heterocycle-fused **NQ** compounds lack this reactivity. These findings underscore the importance of the structural tuning and refinement of the **BQ** moiety in directing the ability of heterocycle-fused **BQ** compounds to change the self-assembly pathways of both metal-free Aβ and metal–Aβ. More importantly, **2a** can covalently cross-link to Aβ *via* **BQ** with the assistance of the benzyl group at the 1-position for Aβ interaction. The **BQ** functionality of **2a** further undergoes *o*-hydroxylation, enhancing its ability to chelate metal ions and, consequently, form a ternary complex with metal–Aβ. Moreover, heterocycle-fused **BQ** compounds simultaneously oxidize multiple amino acid residues in Aβ peptides added with Cu(II) and modify their assembly profiles in both the absence and presence of O_2 to varying degrees. Our compounds ultimately reduce the toxicity induced by Aβ with and without metal ions in living cells. Collectively, our findings highlight the structural variations and optimizations of **BQ** for designing chemical tools to target and control the aggregation and toxicity of both metal-free Aβ and metal–Aβ, as well as developing therapeutic agents to combat metal-entangled pathologies in amyloid diseases. In the near future, detailed structure–activity relationship studies of our compounds will be conducted to identify compounds with the highest efficiency and enhanced properties for biological applications, including metabolic stability and blood–brain barrier permeability, and proceed with their *in vivo* evaluations.

Data availability

All experimental details and data supporting the findings of this study are available within the paper and its ESI.† The data are also available from the corresponding authors upon reasonable request.

Author contributions

Y. Y., H. K., and M. H. L. designed the research. Y. Y. performed gel/western blot, TEM, ESI–MS, docking simulations, and solution speciation studies using Abs spectroscopy and analyzed the data. Y. Y. also conducted cell studies using the MTT assay. K. K. and H. K. synthesized all compounds tested in this work. Y. Y., K. K., H. K., and M. H. L. wrote the manuscript.

Conflicts of interest

There are no conflicts to declare.

Acknowledgements

This work was supported by the National Research Foundation of Korea (NRF) grant funded by the Korean government [RS-2022-NR070709 (M. H. L.)] and the GRRC program [GRRC-KyungHee 2023(B01)] of Gyeonggi province, Republic of Korea (H. K.).

References

1 N. Louros, J. Schymkowitz and F. Rousseau, *Nat. Rev. Mol. Cell Biol.*, 2023, **24**, 912.
2 J. A. Hardy and G. A. Higgins, *Science*, 1992, **256**, 184.
3 E. Karran and B. De Strooper, *Nat. Rev. Drug Discovery*, 2022, **21**, 306.
4 J. Sevigny, P. Chiao, T. Bussiere, P. H. Weinreb, L. Williams, M. Maier, R. Dunstan, S. Salloway, T. Chen, Y. Ling, J. O'Gorman, F. Qian, M. Arastu, M. Li, S. Chollate, M. S. Brennan, O. Quintero-Monzon, R. H. Scannevin, H. M. Arnold, T. Engber, K. Rhodes, J. Ferrero, Y. Hang, A. Mikulskis, J. Grimm, C. Hock, R. M. Nitsch and A. Sandrock, *Nature*, 2016, **537**, 50.
5 M. Sarazin, J. Lagarde, I. El Haddad, L. C. de Souza, B. Bellier, M. C. Potier, M. Bottlaender and G. Dorothee, *Nat. Aging*, 2024, **4**, 761.
6 Y. Zhang, H. Chen, R. Li, K. Sterling and W. Song, *Signal Transduct. Target. Ther.*, 2023, **8**, 248.
7 D. J. Selkoe, *Nat. Aging*, 2024, **4**, 453.
8 M. A. Lovell, J. D. Robertson, W. J. Teesdale, J. L. Campbell and W. R. Markesbery, *J. Neurol. Sci.*, 1998, **158**, 47.
9 J. T. Pedersen, J. Ostergaard, N. Rozlosnik, B. Gammelgaard and N. H. Heegaard, *J. Biol. Chem.*, 2011, **286**, 26952.
10 K. P. Kepp, *Chem. Rev.*, 2012, **112**, 5193.
11 M. G. Savelieff, G. Nam, J. Kang, H. J. Lee, M. Lee and M. H. Lim, *Chem. Rev.*, 2019, **119**, 1221.
12 J.-M. Suh, M. Kim, J. Yoo, J. Han, C. Paulina and M. H. Lim, *Coord. Chem. Rev.*, 2023, **478**, 214978.
13 J. Han, Z. Du and M. H. Lim, *Acc. Chem. Res.*, 2021, **54**, 3930.
14 S. Park, C. Na, J. Han and M. H. Lim, *Metallomics*, 2023, **15**, mfac102.
15 Y. Liu, M. Nguyen, A. Robert and B. Meunier, *Acc. Chem. Res.*, 2019, **52**, 2026.
16 Y. Yi and M. H. Lim, *RSC Chem. Biol.*, 2023, **4**, 121.
17 E. Falcone and C. Hureau, *Chem. Soc. Rev.*, 2023, **52**, 6595.
18 E. Atrián-Blasco, P. Gonzalez, A. Santoro, B. Alies, P. Faller and C. Hureau, *Coord. Chem. Rev.*, 2018, **371**, 38.
19 K. J. Barnham, C. L. Masters and A. I. Bush, *Nat. Rev. Drug Discovery*, 2004, **3**, 205.
20 P. Faller, C. Hureau and O. Berthoumieu, *Inorg. Chem.*, 2013, **52**, 12193.
21 A. I. Bush, *Trends Neurosci.*, 2003, **26**, 207.
22 M. Hong, M. Kim, J. Yoon, S. H. Lee, M. H. Baik and M. H. Lim, *JACS Au*, 2022, **2**, 2001.
23 C. J. Podracky, C. H. An, A. DeSousa, B. M. Dorr, D. M. Walsh and D. R. Liu, *Nat. Chem. Biol.*, 2021, **17**, 317.
24 K. Usui, J. D. Hulleman, J. F. Paulsson, S. J. Siegel, E. T. Powers and J. W. Kelly, *Proc. Natl. Acad. Sci. U. S. A.*, 2009, **106**, 18563.
25 M. Kim, J. Kang, M. Lee, J. Han, G. Nam, E. Tak, M. S. Kim, H. J. Lee, E. Nam, J. Park, S. J. Oh, J. Y. Lee, J. Y. Lee, M. H. Baik and M. H. Lim, *J. Am. Chem. Soc.*, 2020, **142**, 8183.
26 W. Yang, B. S. Kim, Y. Lin, D. Ito, J. H. Kim, Y.-H. Lee and W. Yu, *bioRxiv*, 2021, DOI: 10.1101/2021.08.23.457317.
27 T. Lührs, C. Ritter, M. Adrian, D. Riek-Loher, B. Bohrmann, H. Döbeli, D. Schubert and R. Riek, *Proc. Natl. Acad. Sci. U. S. A.*, 2005, **102**, 17342.
28 D. Eisenberg, E. Schwarz, M. Komaromy and R. Wall, *J. Mol. Biol.*, 1984, **179**, 125.
29 J. S. Derrick, R. A. Kerr, Y. Nam, S. B. Oh, H. J. Lee, K. G. Earnest, N. Suh, K. L. Peck, M. Ozbil, K. J. Korshavn, A. Ramamoorthy, R. Prabhakar, E. J. Merino, J. Shearer, J. Y. Lee, B. T. Ruotolo and M. H. Lim, *J. Am. Chem. Soc.*, 2015, **137**, 14785.
30 M. W. Beck, J. S. Derrick, R. A. Kerr, S. B. Oh, W. J. Cho, S. J. C. Lee, Y. Ji, J. Han, Z. A. Tehrani, N. Suh, S. Kim, S. D. Larsen, K. S. Kim, J. Y. Lee, B. T. Ruotolo and M. H. Lim, *Nat. Commun.*, 2016, **7**, 13115.
31 J. Han, H. J. Lee, K. Y. Kim, G. Nam, J. Chae and M. H. Lim, *Proc. Natl. Acad. Sci. U. S. A.*, 2020, **117**, 5160.
32 Y. S. Lin, W. McKelvey, S. Waidyanatha and S. M. Rappaport, *Biomarkers*, 2006, **11**, 14.
33 N. Uramaru, H. Shigematsu, A. Toda, R. Eyanagi, S. Kitamura and S. Ohta, *J. Med. Chem.*, 2010, **53**, 8727.
34 X. F. Wei, Y. Huang, Z. Karimi, J. P. Qu and B. M. Wang, *J. Org. Chem.*, 2023, **88**, 10190.
35 A. E. Rubtsov, R. R. Makhmudov, N. V. Kovylyaeva, N. I. Prosyanik, A. V. Bobrov and V. V. Zalesov, *Pharm. Chem. J.*, 2002, **36**, 608.
36 A. M. Asiri and S. A. Khan, *Molecules*, 2010, **15**, 6850.
37 V. Boerlin, B. Maeglin, W. Hagler, M. Kuhn and E. Nuesch, *Eur. J. Clin. Pharmacol.*, 1986, **31**, 127.
38 M. Neugebauer, A. Khedr, N. ElRabbat, M. ElKommos and G. Saleh, *Biomed. Chromatogr.*, 1997, **11**, 356.
39 S. Q. Cong, Y. C. Shi, G. J. Yu, F. Zhong, J. J. Li, J. Liu, C. Y. Ye, Z. H. Tan and Y. Deng, *Eur. J. Med. Chem.*, 2023, **250**, 115216.
40 T. Mohamed, A. Shakeri and P. P. N. Rao, *Eur. J. Med. Chem.*, 2016, **113**, 258.
41 V. Esposito, R. Das and G. Melacini, *J. Am. Chem. Soc.*, 2005, **127**, 9358.
42 N. Shu, L. G. Lorentzen and M. J. Davies, *Free Radic. Biol. Med.*, 2019, **137**, 169.
43 Y. L. Han, H. H. Yin, C. Xiao, M. T. Bernards, Y. He and Y. X. Guan, *ACS Chem. Neurosci.*, 2023, **14**, 4051.
44 H. T. T. Phan, K. Samarat, Y. Takamura, A. F. Azo-Oussou, Y. Nakazono and M. C. Vestergaard, *Nutrients*, 2019, **11**, 756.
45 H. Kobayashi, M. Murata, S. Kawanishi and S. Oikawa, *Int. J. Mol. Sci.*, 2020, **21**, 3561.
46 A. S. DeToma, J. Krishnamoorthy, Y. Nam, H. J. Lee, J. R. Brender, A. Kochi, D. Lee, V. Onnis, C. Congiu, S. Manfredini, S. Vertuani, G. Balboni, A. Ramamoorthy and M. H. Lim, *Chem. Sci.*, 2014, **5**, 4851.
47 S. Lee, X. Y. Zheng, J. Krishnamoorthy, M. G. Savelieff, H. M. Park, J. R. Brender, J. H. Kim, J. S. Derrick, A. Kochi, H. J. Lee, C. Kim, A. Ramamoorthy, M. T. Bowers and M. H. Lim, *J. Am. Chem. Soc.*, 2014, **136**, 299.
48 H. J. Lee, K. J. Korshavn, Y. Nam, J. Kang, T. J. Paul, R. A. Kerr, I. S. Youn, M. Ozbil, K. S. Kim, B. T. Ruotolo, R. Prabhakar, A. Ramamoorthy and M. H. Lim, *Chem. Eur. J.*, 2017, **23**, 2706.

49 Y. Yi, J. Han, M. H. Park, N. Park, E. Nam, H. K. Jin, J. S. Bae and M. H. Lim, *Chem. Commun.*, 2019, **55**, 5847.
50 P. I. Eacho, P. S. Foxworthy-Mason, H.-S. Lin, J. E. Lopez, M. K. Mosior and M. E. Richett, *World Intellectual Property Organization*, WO2004093872A1, 2004.
51 T. M. Sokolenko and L. M. Yagupolskii, *Chem. Heterocycl. Compd.*, 2011, **46**, 1335.
52 K. Kim, J. H. Kim, H. Choi, B. Lee, J. Lee, K. M. Ok, T. H. Lee and H. Kim, *Molecules*, 2023, **28**, 6706.
53 K. Okamoto and K. Chiba, *Org. Lett.*, 2020, **22**, 3613.
54 D. R. Appleton, A. N. Pearce and B. R. Copp, *Tetrahedron*, 2010, **66**, 4977.
55 A. Yajima, A. Yamaguchi, F. Saitou, T. Nukada and G. Yabuta, *Tetrahedron*, 2007, **63**, 1080.
56 S. M. Bhosale, A. A. Momin, S. Kunjir, P. R. Rajamohanan and R. S. Kusurkar, *Tetrahedron Lett.*, 2014, **55**, 155.
57 S. M. Bhosale, R. L. Gawade, V. G. Puranik and R. S. Kusurkar, *Tetrahedron Lett.*, 2012, **53**, 2894.
58 H. Kim, T. H. Lee, and H. Lee, Korea Patent, KR2023015005A, 2023.
59 I. Kuperstein, K. Broersen, I. Benilova, J. Rozenski, W. Jonekheere, M. Debulpaep, A. Vandersteen, I. Segers-Nolten, K. Van der Werf, V. Subramaniam, D. Braeken, G. Callewaert, C. Bartic, R. D'Hooge, I. C. Martins, F. Rousseau, J. Schymkowitz and B. De Strooper, *EMBO J.*, 2010, **29**, 3408.
60 S. Sinha, D. H. J. Lopes, Z. M. Du, E. S. Pang, A. Shanmugam, A. Lomakin, P. Talbiersky, A. Tennstaedt, K. McDaniel, R. Bakshi, P. Y. Kuo, M. Ehrmann, G. B. Benedek, J. A. Loo, F. G. Klärner, T. Schrader, C. Y. Wang and G. Bitan, *J. Am. Chem. Soc.*, 2011, **133**, 16958.
61 S. Sinha, D. H. J. Lopes and G. Bitan, *ACS Chem. Neurosci.*, 2012, **3**, 473.
62 A. T. Petkova, R. D. Leapman, Z. H. Guo, W. M. Yau, M. P. Mattson and R. Tycko, *Science*, 2005, **307**, 262.
63 S. Zhang, K. Iwata, M. J. Lachenmann, J. W. Peng, S. Li, E. R. Stimson, Y. Lu, A. M. Felix, J. E. Maggio and J. P. Lee, *J. Struct. Biol.*, 2000, **130**, 130.
64 A. T. Petkova, Y. Ishii, J. J. Balbach, O. N. Antzutkin, R. D. Leapman, F. Delaglio and R. Tycko, *Proc. Natl. Acad. Sci. U. S. A.*, 2002, **99**, 16742.
65 A. T. Petkova, W. M. Yau and R. Tycko, *Biochemistry*, 2006, **45**, 498.
66 N. D. Lazo, M. A. Grant, M. C. Condron, A. C. Rigby and D. B. Teplow, *Protein Sci.*, 2005, **14**, 1581.
67 O. Fónagy, E. Szabó-Bárdos and O. Horváth, *J. Photochem. Photobiol. A*, 2021, **407**, 113057.
68 K. C. Kurien and P. A. Robins, *J. Chem. Soc. B*, 1970, 855, DOI: 10.1039/j29700000855.
69 J. Von Sonntag, E. Mvula, K. Hildenbrand and C. Von Sonntag, *Chem. Eur. J.*, 2004, **10**, 440.
70 M. Inman, A. Visconti, C. Yan, D. Siegel, D. Ross and C. J. Moody, *Org. Biomol. Chem.*, 2014, **12**, 4848.
71 A. Fernández, E. Alvarez, R. Alvarez-Manzaneda, R. Chahboun and E. Alvarez-Manzaneda, *Chem. Commun.*, 2014, **50**, 13100.
72 M. E. Jung and R. W. Brown, *Tetrahedron Lett.*, 1981, **22**, 3355.
73 C. Zhang, Y. Zhang, K. Fan, Q. Zou, Y. Chen, Y. Wu, S. Bao, L. Zheng, J. Ma and C. Wang, *CCS Chem.*, 2022, **4**, 2768.
74 J. Yang, P. Xiong, Y. Shi, P. Sun, Z. Wang, Z. Chen and Y. Xu, *Adv. Funct. Mater.*, 2020, **30**, 1909597.
75 F. Toda, M. Senzaki and R. Kuroda, *Chem. Commun.*, 2002, 1778.
76 C. S. Atwood, R. D. Moir, X. Huang, R. C. Scarpa, N. M. Bacarra, D. M. Romano, M. A. Hartshorn, R. E. Tanzi and A. I. Bush, *J. Biol. Chem.*, 1998, **273**, 12817.
77 W. R. Harris, C. J. Carrano, S. R. Cooper, S. R. Sofen, A. E. Avdeef, J. V. Mcardle and K. N. Raymond, *J. Am. Chem. Soc.*, 1979, **101**, 6097.
78 T. Storr, M. Merkel, G. X. Song-Zhao, L. E. Scott, D. E. Green, M. L. Bowen, K. H. Thompson, B. O. Patrick, H. J. Schugar and C. Orvig, *J. Am. Chem. Soc.*, 2007, **129**, 7453.
79 H. Kim, T. H. Lee, and H. Lee, Korea Patent, KR2022036697A, 2022.
80 Y. Yi, Y. Lin, J. Han, H. J. Lee, N. Park, G. Nam, Y. S. Park, Y. H. Lee and M. H. Lim, *Chem. Sci.*, 2021, **12**, 2456.
81 G. Kim, E. Lelong, J. Kang, J.-M. Suh, N. Le Bris, H. Bernard, D. Kim, R. Tripier and M. H. Lim, *Inorg. Chem. Front.*, 2020, **7**, 4222.
82 D. B. Hibbert and P. Thordarson, *Chem. Commun.*, 2016, **52**, 12792.
83 F. Ulatowski, K. Dabrowa, T. Balakier and J. Jurczak, *J. Org. Chem.*, 2016, **81**, 1746.
84 C. Hureau and P. Dorlet, *Coord. Chem. Rev.*, 2012, **256**, 2175.
85 C. Cheignon, F. Collin, L. Sabater and C. Hureau, *Antioxidants*, 2023, **12**, 472.
86 L. M. Hou, H. Y. Shao, Y. B. Zhang, H. Li, N. K. Menon, E. B. Neuhaus, J. M. Brewer, I. J. L. Byeon, D. G. Ray, M. P. Vitek, T. Iwashita, R. A. Makula, A. B. Przybyla and M. G. Zagorski, *J. Am. Chem. Soc.*, 2004, **126**, 1992.
87 A. A. Watson, D. P. Fairlie and D. J. Craik, *Biochemistry*, 1998, **37**, 12700.
88 M. Friedemann, E. Helk, A. Tiiman, K. Zovo, P. Palumaa and V. Tougu, *Biochem. Biophys. Rep.*, 2015, **3**, 94.
89 M. Gu and J. H. Viles, *Biochim. Biophys. Acta*, 2016, **1864**, 1260.
90 A. K. Nath, A. Ghatak, A. Dey and S. G. Dey, *Chem. Sci.*, 2021, **12**, 1924.
91 G. F. Z. da Silva and L.-J. Ming, *Angew. Chem., Int. Ed.*, 2005, **44**, 5501.
92 M. Kim and M. H. Lim, *Bull. Korean Chem. Soc.*, 2021, **42**, 1272.